Influence of the Mars atmosphere model on aerodynamics of an entry capsule

Gennaro Zuppardi*

*Department of Industrial Engineering – Aerospace Division, University of Naples "Federico II",
Piazzale Tecchio, 80 – 80125 Naples, Italy*

Abstract. This study develops a dual purpose: i) evaluating the effects of two different Mars atmosphere models (NASA Glenn and GRAM-2001) on aerodynamics of a capsule (Pathfinder) entering the Mars atmosphere, ii) verifying the feasibility of evaluating the ambient density and pressure by means of the methods by McLaughlin and Cassanto, respectively and therefore to re-build the values provided by the models. The method by McLaughlin relies on the evaluation of the capsule drag coefficient, the method by Cassanto relies on the measurement of pressure at a point on the capsule surface in aerodynamic shadow. The study has been carried out computationally by means of: i) a code integrating the equations of dynamics of the capsule for the computation of the entry trajectory, ii) a DSMC code for the solution of the flow field around the capsule in the altitude interval 50-100 km. The models show consistent differences at altitudes higher than about 40 km. It seems that the GRAM-2001 model is more reliable than the NASA Glenn model. In fact, the NASA Glenn model produces, at high altitude, temperatures that seem to be too low compared with those from the GRAM-2001 model and correspondingly very different aerodynamic conditions in terms of Mach, Reynolds and Knudsen numbers. This produces pretty different capsule drag coefficients by the two models as well as pressure on its surface, making not feasible neither the method by McLaughlin nor that by Cassanto, until a single, reliable model of the Mars atmosphere is not established. The present study verified that the implementation of the Cassanto method in Mars atmosphere should rely (such as it is currently) on pressure obtained experimentally in ground facilities.

Keywords: Mars atmosphere models; pathfinder capsule; computation of entry trajectory; methods evaluating ambient density and pressure; DSMC method

1. Introduction

It is well known that the success of the exploration of a planet, provided with atmosphere, relies also on the knowledge of the atmosphere parameters. For the survey of the Mars atmosphere, a number of successful missions started longer than 40 years ago and are still today carried on for the detection of its parameters such as the missions: Viking 1 and 2 (both in 1976), Pathfinder (1997), Spirit and Opportunity (both in 2004), Mars Phoenix Lander (2008) and others. Despite these missions, to the author's knowledge, an unique, definitive and completely reliable model for the calculation of the Mars atmosphere parameters seems to be not yet available. On the other hand, the knowledge of these parameters, with particular regard to density, strongly influences the

---

∗Corresponding author, Lecturer, E-mail: zuppardi@unina.it

landing procedure and its technology. For example, the low values of density of the Mars atmosphere makes inefficient the use of parachutes, thus the airbag technology was developed and implemented in Pathfinder, in order to mitigate the impact of the capsule with the soil. It is obvious that the knowledge of these parameters will become even more imperative for the future manned missions; the next frontier of the space exploration is the man's journey to Mars and then its colonization.

Having a reliable atmosphere model makes possible performing reliable calculations both of the entry trajectory and of the aerodynamic quantities of a capsule along the entry path, as per drag coefficient and pressure on the capsule surface. These data can be used, in turn, for correcting density and pressure from the atmosphere model, respectively. Thus a reconstruction of density and pressure can be performed. More specifically according to:

1) McLaughlin *et al.* (2011) and Desai *et al.* (2008), the ambient or the free stream density (ρ_∞) can be evaluated from the measurements of: i) the drag (D), to which the capsule is subjected along the entry path. As the capsule mass (m) is known, the drag can be obtained by the measurement of the capsule deceleration (a) by means of an Inertial Measurement Unit (IMU) installed on the capsule, ii) the free stream velocity (V_∞) by means of telemetric techniques. The atmospheric density can be easily derived from

$$D = ma = \frac{1}{2}\rho_\infty V_\infty^2 C_D S \tag{1}$$

where C_D is the drag coefficient and S is the reference surface. In space applications, the reference surface is the frontal area of the spacecraft. The main cause of uncertainty of this procedure is the drag coefficient. This, in fact, depends on the: shape of the capsule, kind of interaction of the gas molecules with the surface or momentum accommodation coefficients, free stream fluid-dynamic conditions (Mach, Reynolds and Knudsen numbers).

2) Cassanto (1973), Cassanto and Lane (1976), the free stream pressure (p_∞) can be evaluated by means of empirical curves correlating the measured pressure in a point of the surface of a capsule in aerodynamic shadow to the free stream pressure. Cassanto proposed measuring the base pressure (p_b) on the capsule. For safety reasons, in fact, a pressure tap can not be located on the surface exposed to the flow; the presence of holes through the fore-body, or the Thermal Protection System (TPS), is dangerous for the integrity of the capsule. Cassanto evaluated experimentally the ratio p_b/p_∞ by means of ground facilities. The evaluation of the free stream pressure of a planet atmosphere is eventually obtained from the base pressure measured on the capsule during the planet entry and a function correlating the ratio p_b/p_∞. Cassanto deeply analyzed this problem considering the influence of a number of parameters on p_b, such as fore/after-body configuration, free stream Reynolds and Mach numbers, gas composition and so on. Cassanto obtained the correlation formulae (p_b/p_∞) in terms of the free stream Reynolds or Mach numbers. As the success of the procedure is strictly linked to a reliable correlation formula and to accurate measurements of p_b, a preliminary analysis needs to be done for an appropriate location of the pressure tap. In fact, the pressure on a surface in the aerodynamic shadow, which is of the order of magnitude of the free stream one (Cassanto (1973), Cassanto and Lane (1976)), could be below the accuracy of the instrumentation.

The study of aerodynamics in Mars atmosphere started with the Viking missions and is still today in progress, as it can be verified by the large number of papers, relying on computing codes and/or on experimental tests. For example, a number of recent papers are here cited: i) Fei *et al.*

(2016) analyzed, by means of a Direct Simulation Monte Carlo (DSMC) code, the impact of the uncertainties of the Mars atmosphere parameters on hypersonic, rarefied aerodynamics of entry vehicles, ii) Wei *et al.* (2015) analyzed aerodynamics of complex geometry lifting vehicles for precise landing performance during the entry of the Mars Science Laboratory, iii) Desert *et al.* (2017) studied, by means of a 3-D Computational Fluid-Dynamics (CFD) code, aerodynamics of a Martian micro-vehicle, iv) Raju (2015) carried out 2-D CFD computations for evaluating the aerodynamic characteristics of the Phoenix capsules entering the Mars atmosphere at zero angle of attack, v) Viviani and Pezzella (2013), besides performing 3-D CFD computations on a Mars aero-space-plane, evaluated also the effects of chemical reactions, vi) Anyoji *et al.* (2017) and Jiang *et al.* (2018) made tests in wind tunnels besides CFD computations.

The present paper can be considered as a contribution to the long series of papers on the subject "aerodynamics in Mars atmosphere". More specifically, the aim of the present paper is twofold: i) computing the trajectories of a capsule entering the Mars atmosphere by using two different atmosphere models and solving the aerodynamic flow field around the capsule, ii) verifying the feasibility of using the above mentioned methods by McLaughlin and Cassanto.

The present computations considered the Pathfinder capsule (Braun and Manning (2006), Mehta (2011), Williams (2016)) and two atmosphere models, reported in open literature: NASA Glenn (1996), Global Reference Atmosphere Model (GRAM-2001) by Justus and Johnson (2001). The study has been carried out in the altitude interval 50-100 km. Since the rarefaction level of the flow fields from both models in this altitude interval is pretty high, the computations were done by the DSMC code DS2V-4.5 64 bits (Bird (2012)). For the sake of comparison, the atmosphere parameters are also shown for Earth in the altitude interval 0-100 km and the remarkable differences between the two Mars models are pointed out.
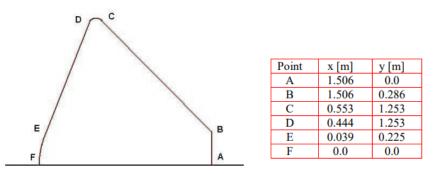

Point	x [m]	y [m]
A	1.506	0.0
B	1.506	0.286
C	0.553	1.253
D	0.444	1.253
E	0.039	0.225
F	0.0	0.0

Fig. 1 Geometrical characteristics of the Pathfinder in the meridian plane (x, y)

Table 1 Pathfinder operative parameters

Type of entry	Direct
Entry velocity	7260 m/s
Entry Path Angle	14.06 deg
Entry mass	585 kg
Touchdown mass	360 kg
Entry ballistic parameter	106 [kg/m^2]
Touchdown ballistic parameter	65 [kg/m^2]
Entry angle of attack	0 deg

2. Mars pathfinder

Mars Pathfinder is an American capsule launched by NASA on December 4, 1996 and landed on Mars on July 4, 1997. Pathfinder carried to Mars a base station with a lightweight (10.6 kg), wheeled robotic Mars rover. The rover conducted a number of experiments on the Mars surface and analyzed the composition of the soil and the morphology of the rocks. Pathfinder carried also scientific instruments and probes for sounding the Mars atmosphere.

Pathfinder is a revolution body whose geometry, in the meridian plane (x, y), is shown in Fig. 1. The curvature radius of the nose, i.e., the curve between points F and E, is 0.664 m. The curvature radius of the rounded shoulder, i.e., the curve between points D and C, is 0.0662 m, the center of curvature is located at x=0.499 m, y=1.206 m. The diameter and the base area surface are: D=2.65 m, S=5.52 m^2, respectively. The heat shield is a 70 deg cone. Pathfinder is provided of a parachute whose opening altitude is 9.4 km. Table 1 summarizes some operative parameters (Braun and Manning (2006)) necessary for the present computations.

3. Mars atmosphere models

Both the NASA Glenn and the Global Reference Atmosphere Model (GRAM-2001) do not provide information about the atmosphere composition. As reported by Williams (2016), the Mars atmosphere is made up of 7 species and its composition is constant with altitude. Table 2 reports both the mass and the molar fractions of each chemical species. Due to dissociation of O_2, N_2 and NO, atomic Oxygen and Nitrogen are also present thus the Mars atmosphere during entry is a mixture of 9 chemical species. For the purpose of the present paper, the chemical model of the Mars atmosphere, used by Bird (2005) in the previous version 3.3 of the DS2V code, has been implemented in the current version of the code. This chemical model relies on 54 reactions: 40 dissociations, 7 forward (or endothermic) exchanges, 7 reverse (or exothermic) exchanges.

According to the NASA Glenn model, pressure decreases exponentially with altitude (h)

$$p = 0.699 \exp(-0.00009 \, h) \tag{2a}$$

and temperature (T) decreases linearly. The Mars atmosphere is divided in two zones: a lower zone up to 7000 m and an upper zone at higher altitudes. Temperature is evaluated by the following equations

$$h \leq 7000 \text{ m: } T = -31 - 0.000998 \, h \tag{2b}$$

$$h > 7000 \text{ m: } T = -23.4 - 0.00222 \, h \tag{2c}$$

where: temperature is in Celsius degrees, pressure is in kilo-Pascal and altitude is in meters. In each zone, density (ρ [kg/m^3]) is computed by the equation of state

$$\rho = p / [0.1921 \, (T + 273.1)] \tag{2d}$$

The GRAM-2001 model is an engineering-oriented model widely used for many Mars mission applications. It is based on the NASA Ames Mars General Circulation Model in the interval 0-80 km and on the Mars Thermosphere General Circulation Model at altitudes above 80 km. Early GRAM-2001 versions were based on "ad hoc" parameterization of data by the Mariner and Viking missions. Recent applications of GRAM-2001 include aero-braking operations of Mars Global
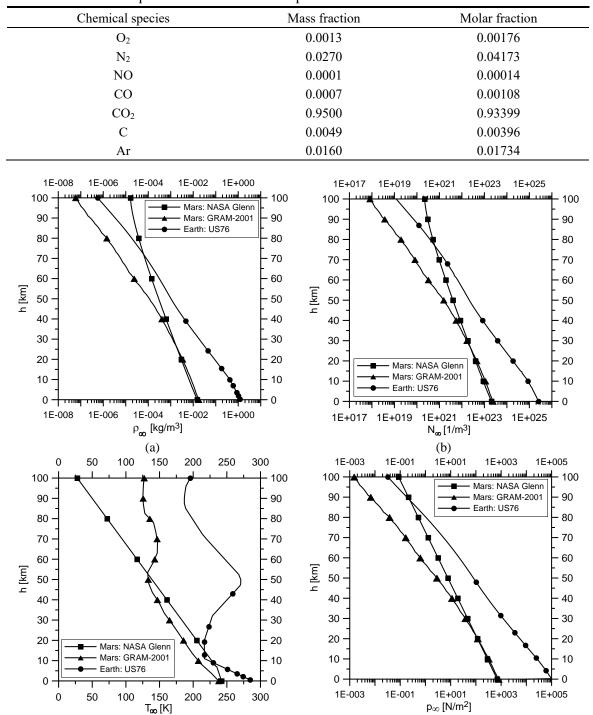
Table 2 Chemical composition of the Mars atmosphere

Chemical species	Mass fraction	Molar fraction
O_2	0.0013	0.00176
N_2	0.0270	0.04173
NO	0.0001	0.00014
CO	0.0007	0.00108
CO_2	0.9500	0.93399
C	0.0049	0.00396
Ar	0.0160	0.01734

Fig. 2 Profiles of density (a), number density (b), temperature (c), pressure and (d) from the Mars and Earth atmosphere models as functions of altitude

Table 3(a) Mars atmosphere parameters at h=0 km

	NASA Glenn	GRAM-2001	US76
T [K]	242	238	288
ρ [kg/m^3]	1.50×10^{-2}	1.73×10^{-2}	1.23
p [N/m^2]	699	779	1.01×10^5
N [1/m^3]	2.06×10^{23}	2.36×10^{23}	2.55×10^{25}

Table 3(b) Mars atmosphere parameters at h=100 km

	NASA Glenn	GRAM-2001	US76
T [K]	28	127	196
ρ [kg/m^3]	1.62×10^{-5}	5.88×10^{-8}	5.63×10^{-7}
p [N/m^2]	8.63×10^{-2}	1.48×10^{-3}	3.22×10^{-2}
N [1/m^3]	2.22×10^{20}	8.05×10^{17}	1.19×10^{19}

Surveyor, prediction and validation of the Pathfinder hypersonic aerodynamics and entry dynamics studies for Mars Polar Lander.

Data used in the present paper (temperature, pressure and density) are those computed and reported by Justus and Johnson (2001). The output is provided in terms of altitude in the interval -1.365÷194.654 km with a step of about 5 km. For the present computations, the parameters at the intermediate altitudes in each step are computed by a linear interpolation.

Figs. 2(a)-2(d) show the profiles of density (a), number density (b), temperature (c), and pressure (d) from the two models as functions of altitude. For the sake of completeness, the profiles of the same quantities for Earth are also shown. The latter are provided by a computer version of the US standard Atmosphere 1976.

The two Mars models are almost equivalent in the altitude interval 0-40 km. For a direct comparison of the models, Tables 3(a) and 3(b) report the values of the parameters at h = 0 and 100 km, respectively. The most evident difference, at h=100 km, is in temperature and correspondingly in density and in number density where the difference is about three orders of magnitude.

4. Pathfinder entry trajectory

The Pathfinder entry trajectory has been computed by the integration of the equations of dynamics of the capsule, already used by Zuppardi and Savino (2015), considering the capsule at zero angle of attack, i.e., with no lift and in free entry, i.e., with no thrusters and with no parachute:

$$\frac{dV}{dh} = \frac{1}{2}\frac{\rho V}{\sin\gamma}\frac{SC_D}{m} - \frac{g}{V} \tag{3a}$$

$$\frac{d\gamma}{dh} = \frac{1}{R\sin\gamma} - \frac{g}{V^2}\frac{1}{tg\gamma} \tag{3b}$$

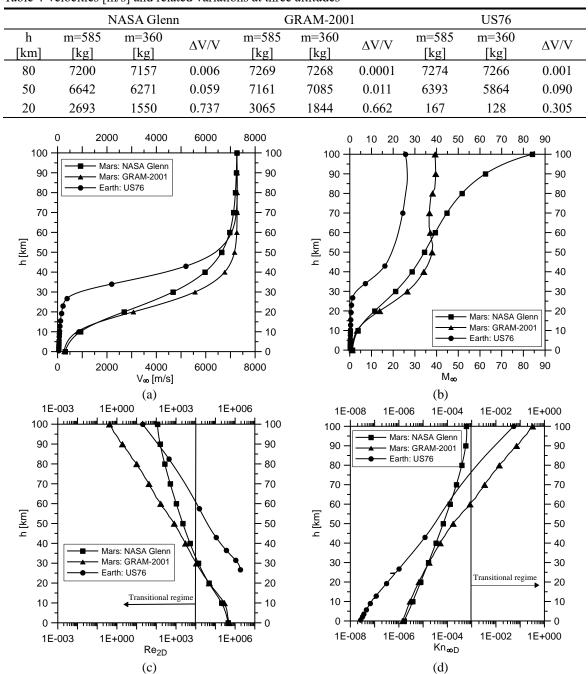where: γ is the flight path angle, g is the gravity acceleration, R is the curvature radius of the

Table 4 Velocities [m/s] and related variations at three altitudes

	NASA Glenn			GRAM-2001			US76		
h [km]	m=585 [kg]	m=360 [kg]	$\Delta V/V$	m=585 [kg]	m=360 [kg]	$\Delta V/V$	m=585 [kg]	m=360 [kg]	$\Delta V/V$
80	7200	7157	0.006	7269	7268	0.0001	7274	7266	0.001
50	6642	6271	0.059	7161	7085	0.011	6393	5864	0.090
20	2693	1550	0.737	3065	1844	0.662	167	128	0.305

Fig. 3 Profiles of velocity (a), Mach number (b), Reynolds number downstream a normal shock wave (c), free stream Knudsen number and (d) along the Mars and Earth atmosphere entry

trajectory and m is the capsule mass. The ratio SC_D/m is the ballistic parameter. Integration started from h=100 km and the step was 0.1 km. The initial data are reported in Tables 1 and 3(b). The

equations have been integrated numerically by a forward scheme with a first order approximation (Euler method). For a preliminary evaluation of the trajectories, the aerodynamic drag coefficient has been assumed to be constant and equal to unit ($C_D=1$).

The trajectories have been preliminary computed to evaluate the influence of the variation of the Pathfinder mass and therefore of the ballistic parameter. As reported in Table 1, due to the heat shield ablation, the Pathfinder mass reduces from 585 kg to 360 kg along the entry trajectory. Once again, for the sake of comparison, a similar analysis was made also for the Earth re-entry trajectory, hypothetically simulating the entry of Pathfinder into the Earth atmosphere. Since the law of mass variation along the trajectory is not known, the calculations of the trajectories have been done at the extreme conditions of m = 585 kg and m = 360 kg. In order to quantify the effect of the mass variation, Table 4 reports the values of velocity (in m/s) at three altitudes using the two masses and the three atmosphere models, as well as the relative variations. At high altitudes, or at altitudes higher than 50 km, the effects of the mass variation is negligible.

Figs. 3(a)-3(d) show the profiles of: free stream velocity (a), free stream Mach number (b), Reynolds number downstream a normal shock wave ($Re_{2D}=\rho_\infty V_\infty D/\mu_2$, c), free stream Knudsen number ($Kn_{\infty D}=\lambda_\infty/D$, d). The very low values of temperature from the Glenn model are responsible for the very high values of the Mach number. For example, at h=100 km M_∞=84 while the Mach number by the GRAM-2001 model is 39. According to: i) Vallerani (1973), the transitional regime for a blunt body is defined, in terms of the Reynolds number downstream a normal shock wave, by $10^{-1}<Re_{D2}<10^4$, ii) Moss (1995) in terms of the global Knudsen number by $10^{-3}<Kn_{D\infty}<50$. In the altitude interval 50-100 km and by both models, Pathfinder can be reasonably considered in continuum low density regime thus the flow field around the Pathfinder has to be solved by means of a DSMC code.

5. Direct simulation Monte Carlo method and DS2V-4.5 64 bits code

The Direct Simulation Monte Carlo (DSMC) method (Bird (1998, 2013) and Shen (2005)) is a statistical and stochastic method, solving flow fields in transitional regime i.e., from the continuum low-density regime to the free molecule regime. DSMC relies on the kinetic theory of gases and considers the gas as made up of millions of simulated molecules, each one representing a large number of real molecules in the physical space (in the present computations between 10^9 and 10^{11}).

The evolution of the molecules, in terms of velocity, spatial coordinates and internal thermodynamic/chemical status, is produced by intermolecular collisions and molecule-surface interactions within the simulated physical space. This is divided into cells both for selecting the colliding molecules and for sampling the thermo-fluid-dynamic quantities. The molecules in a cell represent those at the same location in the physical field. The method does not rely on integration of differential equation therefore it does not suffer from numerical instabilities but is inherently unsteady with a steady solution achievable after a sufficiently long simulation time.

The basic assumption of the method is the temporal decoupling of motion and collision of the simulated molecules. The motion and the collision phases are computed by two distinct algorithms, performed sequentially. This assumption holds when the evolution time step of the aerodynamic system (or global time step), is shorter than the collision time or the time between two subsequent molecular collisions. In the motion phase, the simulated molecules move ballistically at their own velocity over the global time step. Molecules change position in the flow field and interact with the surface of the body under study. In the collision phase, a couple of

colliding molecules are selected in the cell. Chemical reactions take place, both colliding molecules exchange energy among the translational and the interior degrees of freedom (rotation, vibration) and their velocity change. The macroscopic gas properties (density, temperature, etc.) and the macroscopic surface properties (pressure, shear stress, heat flux, etc.) are computed by sampling and then by averaging in each cell and on each surface elemental area, respectively, molecular quantities (number density, gas composition, momentum, kinetic energy, internal energy, etc.) over a pre-fixed number (say 20÷30) of global time steps.

The DSMC code, used in the present study, is the general 2D/axisymmetric code DS2V-4.5 64 bits (Bird (2012)). DS2V-4.5 64 bits is "sophisticated"; in literature, a sophisticated code is labeled also as DSMC07. A DSMC code is defined sophisticated if it implements computing procedures achieving both greater efficiency and accuracy with respect to a "basic" DSMC code; in literature, a basic code is labeled also as DSMC94. More specifically, a DSMC07 code (Bird (2006), Bird *et al.* (2009), Gallis *et al.* (2009)):

1) divides the computational volume into two grids of cells (collision and sampling) with the related cell adaptation. The DS2V-4.5 64 bits code automatically generates the number of cells and the structure of the collision and sampling grids on the basis of the input megabytes (1300 in the present computations) and of the free stream number density. However, the user can change the number of cells and therefore the structure of both grids by inputting the number of molecules for the adaptation of the collision and of the sampling cells; the lower the input number of molecules per cell, the higher the number of cells after the adaptation process,

2) implements the "nearest neighbor" procedure for the selection of the pair of colliding molecules in the collision cell. This procedure is aimed at fulfilling the physical condition that a molecule collides with the molecule closest to it. This implies that, when a molecule is chosen at random in the collision cell, the collision partner is the molecule closest to it. In the DSMC94 method, the collision partner was selected at random in the same computing cell,

3) provides an optimal global time step. This is computed as a fraction (say 0.2) of the current, collision time, averaged over the computing dominion. In the DSMC94 method, the global time step was an input to the code and then kept constant during the evolution of the system, therefore irrespective of the actual, evolving fluid-dynamic conditions,

4) avoids sequential collisions between the same collision pair. This procedure does not allow a second collision between the same collision partners; this is, in fact, physically impossible because after a collision, the molecules move away in opposite directions,

5) allows the user to state the quality of a computation by means of the evaluation of the adequacy of the numbers of simulated molecules and of collision cells. The ratio between the molecule mean collision separation (mcs) and the mean free path (λ), in each collision cell, is the parameter making possible this evaluation; mcs/λ has to be less than unity everywhere in the computational domain for a good quality of a DSMC computation. Bird (2006) suggests that the mcs/λ ratio should be less than 0.2 for an optimal quality of the computation.

6) provides indication about the stabilization of the computation. Stabilization is achieved when the profile of the number of the simulated molecules, as a function of the simulated time, becomes jagged and included within a band which defines the standard deviation of the number of simulated molecules.

6. Test conditions, computation parameters and quality of the results

The analysis relies on 22 DS2V computations: 11 altitudes between 50 and 100 km with a

spacing of 5 km and 2 Mars atmosphere models. All computations considered the molecule/surface interaction fully accommodated and the surface non-catalytic.

Tables 5(a) and 5(b) report for the two models and for each altitude: i) input data to DS2V, i.e., free stream velocity V_∞, number density N_∞, temperature T_∞, ii) computation parameters, i.e., number of simulated molecule N_m, number of real molecules represented by each simulated molecule F_N, number of sampling cells N_S, number of collision cells N_C, iii) parameters quantifying the quality of the results i.e., ratios of mean collision separation on mean free path mcs/λ and of simulation time on the fluid-dynamic time t_s/t_f. The fluid dynamic time is calculated as the time necessary to the fluid to cross the length (L) of the body under study (in this case L = 1.506 m, see Fig.1) at the free flow velocity: $t_f = L / V_\infty$.

For both models, the computing parameters do not change meaningfully with altitude, while the best values of the parameters, quantifying the quality of the results (i.e., the lowest values of mcs/λ and the highest values of t_s/t_f), are obtained by the GRAM-2001 model. This is due to the lower

Table 5(a) Input data, computation parameters, quality of the results parameters: Glenn model

H [km]	V_∞ [m/s]	N_∞ [1/m³]	T_∞ [K]	N_m	F_N	N_S	N_C	mcs/λ	t_s/t_f
100	7260	2.22×10^{20}	28	3.60×10^7	5.87×10^{10}	8.43×10^4	1.91×10^6	0.084	5.54
95	7250	2.48×10^{20}	39	3.59×10^7	6.57×10^{10}	8.42×10^4	1.88×10^6	0.093	5.28
90	7238	3.03×10^{20}	50	3.62×10^7	8.02×10^{10}	9.37×10^4	2.18×10^6	0.115	5.46
85	7222	3.88×10^{20}	61	3.57×10^7	1.03×10^{11}	9.55×10^4	2.11×10^6	0.148	4.82
80	7200	5.15×10^{20}	72	3.49×10^7	1.36×10^{11}	9.56×10^4	2.00×10^6	0.197	4.16
75	7169	7.01×10^{20}	83	3.58×10^7	1.85×10^{11}	9.11×10^4	1.95×10^6	0.269	4.69
70	7125	9.69×10^{20}	94	3.45×10^7	2.57×10^{11}	9.28×10^4	1.83×10^6	0.380	3.82
65	7062	1.36×10^{21}	105	3.31×10^7	3.60×10^{11}	9.15×10^4	1.68×10^6	0.546	3.16
60	6969	1.93×10^{21}	117	3.58×10^7	3.83×10^{11}	8.49×10^4	2.03×10^6	0.666	3.43
55	6836	2.76×10^{21}	128	3.28×10^7	5.48×10^{11}	9.36×10^4	2.30×10^6	1.031	2.12
50	6642	3.99×10^{21}	139	3.17×10^7	7.91×10^{11}	9.07×10^4	2.14×10^6	1.528	2.20

Table 5(b) Input data, computation parameters, quality of the results parameters: GRAM-2001 model

H [km]	V_∞ [m/s]	N_∞ [1/m³]	T_∞ [K]	N_m	F_N	N_S	N_C	mcs/λ	t_s/t_f
100	7260	8.05×10^{17}	127	3.84×10^7	3.20×10^8	9.03×10^4	1.15×10^6	0.0004	10.9
95	7262	1.64×10^{18}	126	3.25×10^7	6.50×10^8	8.09×10^4	2.36×10^6	0.0008	10.4
90	7265	3.66×10^{18}	125	3.54×10^7	1.12×10^9	8.62×10^4	2.46×10^6	0.002	15.0
85	7267	8.61×10^{18}	127	4.09×10^7	2.02×10^9	1.20×10^5	2.50×10^6	0.001	12.9
80	7269	1.94×10^{19}	135	3.10×10^7	5.92×10^9	8.28×10^4	2.17×10^6	0.007	11.8
75	7269	4.08×10^{19}	143	3.22×10^7	1.25×10^{10}	8.78×10^4	2.19×10^6	0.015	10.9
70	7268	8.09×10^{19}	146	3.21×10^7	2.47×10^{10}	8.76×10^4	2.10×10^6	0.030	8.20
65	7264	1.56×10^{20}	147	3.14×10^7	4.76×10^{10}	8.37×10^4	1.97×10^6	0.057	6.10
60	7253	3.20×10^{20}	143	3.18×10^7	9.76×10^{10}	8.45×10^4	1.85×10^6	0.120	5.81
55	7226	7.13×10^{20}	135	3.07×10^7	2.18×10^{11}	8.37×10^4	1.61×10^6	0.280	4.23
50	7161	1.53×10^{21}	133	2.79×10^7	4.68×10^{11}	8.20×10^4	1.34×10^6	0.641	2.70

values of density and therefore of the number density (see Figs.2(a), 2(b)), compared with those by the Glenn model; decreasing the free stream number density favors any DSMC calculation and improves the related quality of the results. Even though the computations with the Glenn model at h=50 and 55 km should not be rigorously accepted (mcs/λ are lightly higher than 1) however, for the sake of completeness, the results have been included in the present analysis.

7. Analysis of results

Fig. 4(a) shows the profiles of the Pathfinder drag as functions of altitude. As expected, the higher values of the free stream density by the NASA Glenn model, compared with those by the GRAM-2001 model, produce higher values of the aerodynamic drag. On the contrary, the drag coefficients by both models (Fig. 4(b)) do not show significant differences up to an altitude of 75 km; the difference is on the second decimal digit. The difference between the models starts from 75 km and increases with altitude; this is due to the very different fluid-dynamic conditions or Mach, Reynolds and Knudsen numbers. For a direct comparison, Tables 6(a) and 6(b) report the values of: drag, drag coefficient, free stream Mach, Reynolds and Knudsen numbers from the two models at the altitudes of 50, 65, 80, 90 and 100 km. The Mach number by the Glenn model increases strongly with altitude while the Reynolds and Knudsen numbers do not change meaningfully. An opposing fluid-dynamic condition occurs for the GRAM-2001 model. The much lower values of the Reynolds number by the GRAM-2001 model involve higher values of the drag coefficient.

The small variability of C_D with altitude by the Glenn model facilitates the use of the following polynomial, best-fit curve for the evaluation of C_D as function of altitude

NASA Glenn, $50 \leq h \leq 100$ km:

$$C_D = 1.5796 - 1.2202 \times 10^{-3}\, h + 1.7538 \times 10^{-5}\, h^2 - 9.3294 \times 10^{-8}\, h^3 \qquad (4a)$$

Interpolation of the drag coefficients from GRAM-2001 model is fulfilled by means the two following best fit curves

GRAM-2001, $50 \leq h \leq 75$ km:

$$C_D = 2.0648 - 2.3228 \times 10^{-2}\, h + 3.4533 \times 10^{-4}\, h^2 - 1.7340 \times 10^{-6}\, h^3 \qquad (4b)$$

GRAM-2001, $75 < h \leq 100$ km:

$$C_D = 12.6941 - 4.4824 \times 10^{-1}\, h + 5.7542 \times 10^{-3}\, h^2 - 2.3524 \times 10^{-5}\, h^3 \qquad (4c)$$

where h is in km. The correlation coefficients are high enough: 0.9975 for Eq. (4a), 0.9830 for Eq.(4b) and 0.9946 for Eq.(4c).

As mentioned in the Introduction, Eqs.(4a, 4b, 4c) can be used for the correction of density, provided by the atmosphere models and for refining the calculation of the entry trajectories, as well. For example, Figs. 5(a) and 5(b) show for both models the comparison of the profiles of the entry velocity, computed both with constant, unitary drag coefficient (C_D=1) and with variable drag coefficient (C_D= C_D(h)) and, for the sake of completeness, also of a characteristic number as per the Reynolds number. The influence of a variable drag coefficient seems to be negligible for both models. For this reason, the data shown below are those calculated with C_D=1.
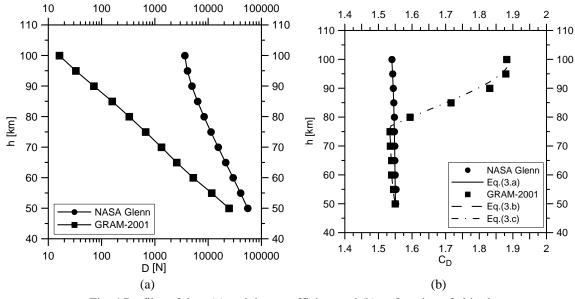
Fig. 4 Profiles of drag (a) and drag coefficient and (b) as function of altitude

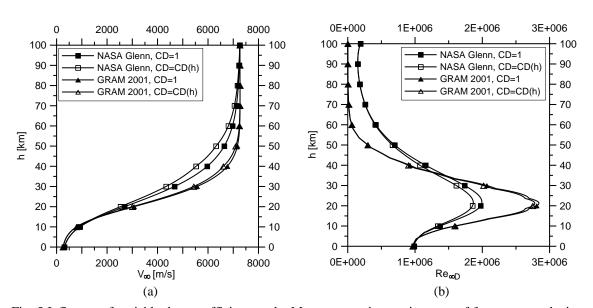Table 6(a) Pathfinder drag and drag coefficient, free stream Mach, Reynolds and Knudsen numbers from the Glenn model

h [km]	D [N]	C_D	M_∞	$Re_{\infty D}$	$Kn_{\infty D}$
100	3.63×10^3	1.54	84.1	1.90×10^5	6.04×10^{-4}
90	4.94×10^3	1.54	62.5	1.49×10^5	5.69×10^{-4}
80	8.33×10^3	1.55	51.7	1.80×10^5	3.92×10^{-4}
65	2.12×10^4	1.55	41.9	3.27×10^5	1.75×10^{-4}
50	5.50×10^4	1.55	34.4	6.98×10^5	6.71×10^{-5}

Table 6(b) Pathfinder drag and drag coefficient, free stream Mach, Reynolds and Knudsen umbers from the GRAM-2001 model

h [km]	D [N]	C_D	M_∞	$Re_{\infty D}$	$Kn_{\infty D}$
100	1.61×10^1	1.88	39.3	1.67×10^2	3.20×10^{-1}
90	7.12×10^1	1.83	39.5	7.68×10^2	7.01×10^{-2}
80	3.29×10^2	1.59	38.1	3.80×10^3	1.37×10^{-2}
65	2.55×10^3	1.54	36.6	2.83×10^4	1.76×10^{-3}
50	2.45×10^4	1.55	37.9	3.00×10^5	1.72×10^{-4}

For an entry capsule, pressure (p(0)) and heat flux ($\dot{q}$ (0)) at the capsule stagnation point are important aerodynamic parameters. These parameters, in fact, can heavily influence the structural design of the TPS. Figs. 6(a) and 6(b) show the profiles of p(0) and of the related coefficient $C_p(0)$. Figs. 7(a) and 7(b) show the profiles of $\dot{q}$ (0) and the related coefficient $C_h(0)$, all as functions of altitude for both models. These profiles are similar to those of drag and of drag coefficient (see

Fig. 5 Influence of variable drag coefficient on the Mars entry trajectory in terms of free stream velocity (a) and free stream Reynolds number (b)
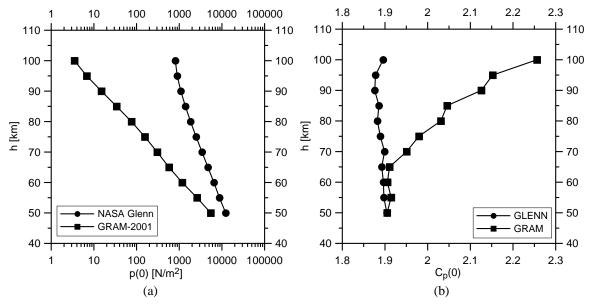

Fig. 6 Profiles of pressure (a) and pressure coefficient and (b) at the Pathfinder stagnation point as functions of altitude

Fig. 4(a) and 4(b)). The values of p(0) and $\dot{q}(0)$ for the Glenn model are higher than those from the GRAM-2001 model. This had to be expected because strictly linked to higher values of the free stream dynamic pressure $(\rho_\infty V^2_\infty)$ and kinetic energy flux $(\rho_\infty V^3_\infty)$ of the Glenn model. For example for a direct quantification, Tables 7(a) and 7(b) report the values of p(0), Cp(0), $\dot{q}(0)$, Ch(0), $(\rho_\infty V^2_\infty)$ and $(\rho_\infty V^3_\infty)$ the two models at h=50 and 100 km.
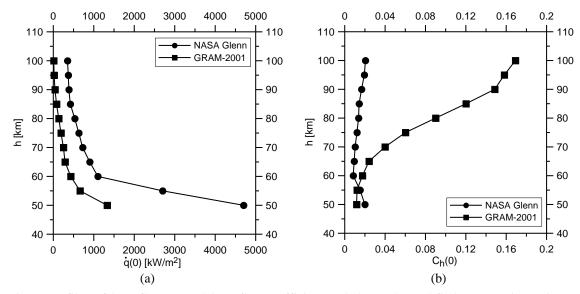
Fig. 7 Profiles of heat flux (a) and heat flux coefficient and (b) at the Pathfinder stagnation point as functions of altitude

Table 7(a) Pressure and heat flux at the capsule stagnation point: GLENN model

h [km]	$p(0)$ [N/m^2]	$\rho_\infty V_\infty^2$ [N/m^2]	$C_p(0)$	$\dot{q}(0)$ [kW/m^2]	$\rho_\infty V_\infty^3$ [kW/m^2]	$C_h(0)$
100	8.10×10^2	8.54×10^2	1.90	3.50×10^2	6.20×10^6	0.02
50	1.23×10^4	1.29×10^4	1.90	4.70×10^3	8.54×10^7	0.02

Table 7(b) Pressure and heat flux at the capsule stagnation point: GRAM 2001 model

h [km]	$p(0)$ [N/m^2]	$\rho_\infty V_\infty^2$ [N/m^2]	$C_p(0)$	$\dot{q}(0)$ [kW/m^2]	$\rho_\infty V_\infty^3$ [kW/m^2]	$C_h(0)$
100	3.50	3.10	2.26	1.05×10^1	2.25×10^4	0.169
50	5.47×10^3	5.74×10^3	1.90	1.33×10^3	4.11×10^7	0.012

The DSMC simulations provide useful information about the localization of the pressure tap on the capsule surface in areas in aerodynamic shadow. Fig. 8(a) shows the pressure profiles along the Pathfinder surface computed by both models at the extreme altitudes of 50 and 100 km. Figure clearly shows also that the measurement of the base pressure, i.e., the measurement of the pressure on the surface between points A and B (see Fig. 1), as suggested by Cassanto, seems to be not feasible because the computed pressure is almost zero even at h=50 km. This can be verified also by Figs. 8(b) and 8(c), showing the 2-D maps of pressure in the flow field around Pathfinder at the intermediate altitude of h=75 km computed by the GRAM-2001 model (Fig. 8(b)) and by the Glenn model (Fig. 8(c)), respectively. The stream lines pattern clearly verifies a flow recirculation at the base surface of Pathfinder (zone A-B) and that the flow is attached near point C (the coordinates of points A thru F are reported in Fig.1). Thus, the positioning of the pressure tap on the frustum after-body was assumed at x=0.60 m (s=1.53 m), i.e., only slightly downstream point C. For this reason, the pressure at this point will be labeled as p_C.
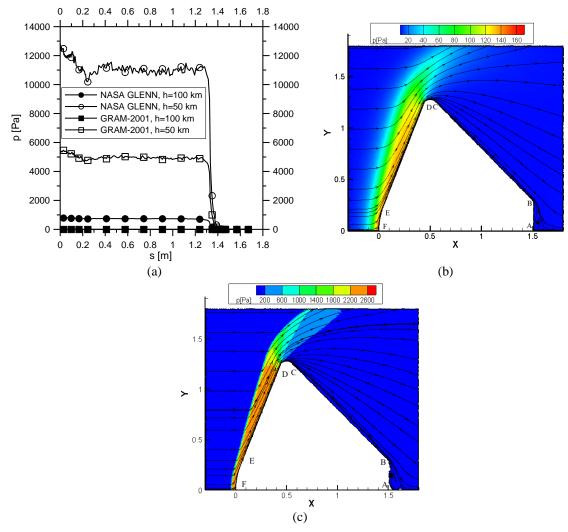
(a)

(b)

(c)

Fig. 8 Pressure distribution on the Pathfinder surface (a), 2-D maps of pressure and stream lines pattern in the meridian plane of Pathfinder from the GRAM-2001 (b) and the Glenn model (c) at h=75 km

Fig. 9(a) shows the profiles of pressure (p_C) as functions of altitude. As reported by Russo (2011), the current pressure sensors are able to measure, in laboratory, very low pressures even up to 10^{-9} [Pa]. Therefore, measuring a pressure (p_C) of about 4×10^{-4} [Pa] even though on a capsule "flying" in space therefore in a difficult situation, seems to be reasonable, hence the Cassanto method could be used in the whole altitude range for re-building the values of pressure computed by both models. Eqs. 4(a), 4(b) and 4(c) are the polynomial curves best fitting the ratio p_C/p_∞ as functions of altitude. Eq. 4(a) interpolates p_C/p_∞ by the Glenn model as functions of altitude in the whole altitude range. Eqs. 4(b) and 4(c) interpolate p_C/p_∞ by the GRAM-2001 model in the altitude range 50-80 km and 80-100, respectively. The present computations verify the condition, reported by Cassanto (1973) and Cassanto and Lane (1976), that the pressure in areas of the capsule in aerodynamic shadow is of the same order of magnitude of the ambient pressure ($p_C/p_\infty\equiv O(1)$).
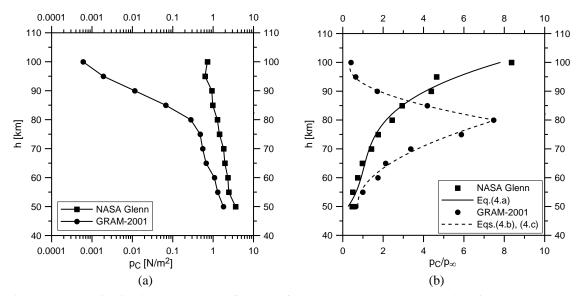
Fig. 9 Pressure distributions on the Pathfinder surface at x=0.60, y=1.20 (a), ratio of p_C/p_∞ and (b) as functions of altitude

NASA Glenn, 50≤h≤100 km:

$$p_C/p_\infty = -30.1155 + 1.3962\ h - 2.1378 \times 10^{-2}\ h^2 + 1.1208 \times 10^{-4}\ h^3$$

(5a)

GRAM-2001, 50≤h≤80 km:

$$p_C/p_\infty = 21.3086 - 0.8105\ h + 7.9862 \times 10^{-3}\ h^2$$

(5b)

GRAM-2001, 80≤h≤100 km:

$$p_C/p_\infty = 207.9087 - 4.2265\ h + 2.1516 \times 10^{-2}\ h^2$$

(5c)

where h is in km. The correlation coefficient are high enough also for these best fit curves: 0.9853 for Eq. (5a), 0.9939 for Eq. (5b) and 0.9997 for Eq. (5c). Being the correlation formulae substantially different and strongly dependent on the atmosphere model, the use of these formulae is impractical for implementing the Cassanto method in the altitude interval 50 and 100 km. Therefore the implementation of the Cassanto method should rely, as it is currently, on correlation formulae obtained experimentally in ground facilities.

7. Conclusion

The influence of the Mars atmosphere models NASA Glenn and GRAM-2001 have been evaluated both on the entry trajectory, computed by a code integrating the equations of dynamics of a capsule, and on the solution of the flow field around the capsule Mars Pathfinder with the computation of aerodynamic parameters by means of the DSMC code DS2V-4.5 64 bits.

The models showed consistent difference at altitudes higher than about 40 km. For this reason

the aerodynamic analysis has been carried out in the altitude interval 50-100 km. It seems that the GRAM-2001 model is more reliable than the NASA Glenn model. In fact, a linear decrease in temperature with altitude for the NASA Glenn model is not realistic, because producing, at high altitude, excessively low temperatures with corresponding high density. This generates, in turn, fluid-dynamic conditions or numbers of Mach, Reynolds and Knudsen very different from those by the GRAM-2001 model.

The feasibility of correcting the ambient density and pressure by the models, by means of the methods by McLaughlin and by Cassanto was also evaluated. The very different fluid-dynamic conditions by the two models generated very different values of both drag coefficients of Pathfinder and pressure on its surface, making not feasible both methods. The effective reconstruction and refinement of the Mars atmosphere density and pressure from both methods is entrusted to when a single, reliable Mars atmosphere model will be available. Therefore until then, the implementation of the Cassanto method should rely, as it is currently, on correlation formulae obtained experimentally in ground facilities.

References

Anyoji, M., Okamoto, M., Fujita, K., Nagai, H. and Oyama, A. (2017), "Evaluation of aerodynamic performance of Mars airplane in scientific balloon experiment", *Fluid Mech*. *Res*. *Int*., **1**(3), 1-7. https://doi.org/10.15406/fmrij.2017.01.00012.

Bird, G.A. (1998), *Molecular Gas Dynamics and Direct Simulation Monte Carlo Method*, Clarendon Press, Oxford, U.K.

Bird, G.A. (2005), *Visual DSMC Program for Two-Dimensional Flows*, DS2V Program User's Guide Ver. 3.3, G.A.B. Consulting Pty Ltd, Sydney, Australia

Bird, G.A. (2006), "Sophisticated versus simple DSMC", *Proceedings of the 25th International Symposium on Rarefied Gas Dynamics*, Saint Petersburg, Russia, July.

Bird, G.A., Gallis, M.A., Torczynski, J.R. and Rader, D.J. (2009), "Accuracy and efficiency of the sophisticated direct simulation Monte Carlo algorithm for simulating non-continuum gas flows", *Phys. Fluids*, **21**(1), https://doi.org/10.1063/1.3067865.

Bird, G.A. (2012), *Visual DSMC program for Two-Dimensional Flows*, DS2V Program User's Guide, Ver. 4.5., G.A.B. Consulting Pty Ltd, Sidney, Australia.

Bird, G.A. (2013), *The DSMC Method, Version 1.1*, Amazon, ISBS 9781492112907, Charleston, U.S.A.

Braun, R.D. and Manning, R.M. (2006), "Mars exploration entry, descent and landing challenges", IEEE 0075, 1-32.

Cassanto, J.M. (1973), "A base pressure experiment for determining the atmospheric pressure profile of planets", *J. Spacecraft*, **10**(4), 253-261. https://doi.org/10.2514/3.61875.

Cassanto, J.M. and Lane, J.W. (1976), "A high-altitude base pressure experiment", *AIAA J*., **14**(8), 1050-1053. https://doi.org/10.2514/3.61440.

Desai, P.N., Prince, J.L., Queen, E.M., Cruz, J.R. and Grover, M.R. (2008), "Entry, descent, and landing performance of the mars phoenix lander", *J. Spacecraft Rockets*, **48**(5), 798-808. https://doi.org/10.2514/1.48239.

Desert, T., Moschetta, J.M. and Bezard, H. (2017), "Aerodynamic design of a Martian micro air vehicle", *Proceedings of the 7th European Conference for Aeronautics and Aerospace Sciences*, Milan, Italy, July.

Fei, H., Jin, X.H.., Lv, J.M. and Cheng, X.L. (2016), "Impact of Martian parameter uncertainties on entry vehicles aerodynamics for hypersonic rarefied conditions", *AIP Conference Proc*., **1786**, 190006.

Gallis, M.A., Torczynski, J.R., Rader, D.J. and Bird, G.A. (2009), "Convergence behavior of a new DSMC algorithm", *J. Comput. Phys*., **228**(12), 4532-4548. https://doi.org/10.1016/j.jcp.2009.03.021.

Jiang, H., Liu, X., Han, G. and Chen, X. (2018), "Hypersonic simulation of Mars entry atmosphere based on

gun tunnel", *Proceedings of the 5ᵗʰ International Conference on Experimental Fluid Mechanics (ICEFM 2018)*, Munich, Germany, July.

Justus, C.G. and Johnson, D.L. (2001), *Mars Global Reference Atmospheric Model 2001 (Mars-GRAM 2001) User Guide*, NASA TM 2001-210961.

McLaughlin, C.A., Mance, S. and Lechtenberg, T. (2011), "Drag coefficient estimation in orbit determination", *J. Astronaut. Sci*., **58**(3), 513-530. https://doi.org/10.1007/BF03321183.

Mehta, R.C. (2011), "Computations of flow field over re-entry modules at high speed", *Comput. Simul. Appl.*, http://www.intechopen.com/articles/show/title/computations-of-flowfield-over-reentry-modules-at-high-speed.

Moss, J.N. (1995), "Rarefied flows of planetary entry capsules", AGARD-R-808, 95-129, Special course on "Capsule aerothermodynamics", Rhode-Saint-Genèse, Belgium.

NASA Glenn Research Center (1996), *Mars Atmosphere Model*, file:///C:/MARS/MARS-ATMOSPHERE/Mars%20Atmosphere%20Model%20%20Metric%20Units.htm.

Raju, M. (2015), "CFD analysis of Mars Phoenix capsules at Mach number 10", *J. Aeronaut. Aerospace Eng*., **4**(1), 1-4.

Russo, G.P. (2011), *Aerodynamic Measurements: from Physical Principles to Turnkey Instrumentation*, 1st Edition, Woodhead Publishing Limited, Suffolk, U.K.

Shen, C. (2005), *Rarefied Gas Dynamic: Fundamentals, Simulations and Micro Flows*, Springer-Verlag, Berlin, Germany.

Vallerani, E. (1973), "A review of supersonic sphere drag from the continuum to the free molecular flow regime", AGARD CPP 124, Paper 22, 1-15.

Viviani, A. and Pezzella, G. (2013), "Non-equilibrium computational flowfield analysis for the design of Mars manned entry vehicles", *Prog. Flight Phys*., **5,** 493-516.

Tang, W., Yang, X.F., Gui, Y.W. and Du, Y.X. (2015), "Aerodynamic prediction and performance analysis for mars science laboratory entry vehicle", *Int. J. Aerospace Mech. Eng*., **9**(6), 1040-1045.

Williams, D.R. (2016), "Mars fact sheet", https://nssdc.gsfc.nasa.gov/planetary/factsheet/marsfact.html.

Zuppardi, G. and Savino, R. (2015), "DSMC aero-thermo-dynamic analysis of a deployable capsule for mars atmosphere entry", *Proceedings of the DSMC15 Conference*, Kauai, Hawaii, U.S.A., September.

EC